RECEIVED
LAWRENCE
RADIATION LABORATORY
JUL 12 1971
LIBRARY AND
DOCUMENTS SECTION

UCRL-20664 c.2
UC-34 Physics
TID-4500 (57th Ed.)

MONITORING OF POSITIVELY CHARGED PARTICLES IN THE ELECTRON RING ACCELERATOR

K. Goebel, J. B. McCaslin, H. W. Patterson, and A. R. Smith

April 1971

AEC Contract No. W-7405-eng-48

TWO-WEEK LOAN COPY

This is a Library Circulating Copy which may be borrowed for two weeks. For a personal retention copy, call Tech. Info. Division, Ext. 5545

LAWRENCE RADIATION LABORATORY
UNIVERSITY of CALIFORNIA BERKELEY

UCRL-20664 c.2

34

MONITORING OF POSITIVELY CHARGED PARTICLES IN THE ELECTRON RING ACCELERATOR

K. Goebel, J. B. McCaslin, H. W. Patterson, and A. R. Smith

Lawrence Radiation Laboratory
University of California
Berkeley, California 94720

April 1971

ABSTRACT

Some methods for beam monitoring of protons and heavy ions at the ERA are discussed in terms of sensitivity and susceptibility to interference from competing reactions. Results presented of a pilot exposure at the 88-inch cyclotron compare calculated and measured production rates of ^{149}Tb and ^{151}Tb from bombardment of a cerium target with 55.48-MeV nitrogen ions. From this work we conclude that at least 10^{11} ions (@ 5 MeV/amu) are needed to produce a measurable amount of alpha activity.

Introduction

The electron-ring or collective-effect accelerator uses dense charge clusters of electrons, which produce larger fields than are normally produced externally, in order to accelerate positively charged particles. Ions trapped in these self-fields gain energy at a rate determined by the ratio of the mass of the ion to that of the electron.[1]

Initially, we are concerned with the detection and measurement of protons of 4 to 5 MeV in the presence of much larger numbers of electrons of 15 to 20 MeV. Interference from electrons, bremsstrahlung radiation, and neutrons may pose severe problems in making measurements of the positively charged component of the beam by conventional methods.

Nuclear reactions induced by the positively charged particles may be used as an independent or alternative monitoring method. This report deals briefly with some of the possible reactions for measuring protons in the energy region of a few MeV, and discusses in more detail some monitoring methods for heavy ions.

A. MONITOR REACTIONS FOR PROTONS

1. (p^+, f) Reactions

Cross sections of the proton-induced fission reactions in heavy elements decrease rapidly below the Coulomb barrier (10 to 20 MeV), and are, at 4 MeV (according to the measurements made by Choppin et al.[2]), as low as 2 μb for ^{232}Th and 4 to 5 μb for ^{238}U. (See Fig. 1.) These measurements agree rather well with those by Tewes and James[3] for energies between 6 and 21 MeV, with those by Butler et al.[4] for 6 to 7 MeV, and

with those by Jones et al.[5] for energies between 12 and 20 MeV.

At the low proton energies, however, with which we are concerned at ERA, we must exclude proton-induced fission reactions as possible monitors because of the competing gamma- and neutron-induced fission reactions, which have cross sections 10^4 to 10^5 times as high.[6] (See Figs. 2 and 3.)

2. ^{7}Li(p, γ) ^{8}Be

This reaction evokes great initial interest because of the high energy of the γ ray (17.6 MeV) resulting from it. We calculate that, using this reaction, we could detect one event per ERA beam burst, assuming the following conditions:

- 10% detection efficiency for a 4×4-in. NaI(Tl) crystal, totalling under the photopeak and the first and second escape peaks,
- isotropic γ-ray emission,[7]
- geometry factor 10^{-3} ($10^{-3} \times 4\pi$ sr),
- average cross section 1 mb,
- beam intensity 10^{10} p^+ per pulse.

As the ERA burst lasts only about 5 nsec, the maximum number of events that could be registered with a single detector is limited to one event per burst.

A Cerenkov counter used for this purpose would have the advantage of fast response, which can be used to discriminate against the high background from bremsstrahlung. The electron-produced bremsstrahlung spectrum will extend up to 20 MeV, but the electrons are lost earlier near the trim coils, whereas the protons travel further down to a LiF target placed about 3 ft downstream from the electron loss point. The bremsstrahlung quanta would reach the detector with the velocity of light and within negligible time spread, but the protons having about 0.1 c would hit the target about 30 nsec later, thus allowing the counter to be gated off during the period of high bremsstrahlung background. Further, in a lead glass Cerenkov counter the directional response could be used for selecting γ rays from the proper direction. According to our estimates of bremsstrahlung intensity the detectors would have to be shielded by 20 cm of lead, corresponding to a shielding factor of 10^6 at 10 MeV/photon.

Figure 4 shows the excitation function for ^{7}Li(p, γ)^{8}Be at low proton energies.[7,8] Appropriate pre-absorbers would have to be used to define the proton energy because the reaction has a low threshold at about 100 keV.

3. (p, n) Reactions

We have selected some (p, n) reactions with low threshold energies leading to isotopes with suitable half-lives and decay schemes. The reaction products listed in Table I are all positron emitters. These isotopes could be counted outside the ERA vacuum; it would be, however, much easier to do the counting inside in some lateral extension of the vacuum system to which the target could be transferred remotely. In this way the detector would be somewhat remote from the accelerator axis, and could be shielded to prevent radiation damage. Near the point of electron impact the dose rate is estimated to be 10^4 to 10^5 rads per pulse.

As an example we consider the first reaction listed in Table I, for which Fig. 5 shows the measured ^{11}B(p, n)^{11}C excitation function. After a steep rise at 3.1 MeV, the cross section remains constant at about 15 mb/sr up to 5 MeV. However, there are some competing reactions which could also produce ^{11}C. ^{10}B(p, γ)^{11}C has a threshold at about 0.8 MeV, as shown in Fig. 6. The cross section is much lower, and the isotopic abundance of ^{10}B is only about 20%, but with a high proton flux a misinterpretation with respect to energy is possible. The same

applies to the $^{10}B(d,n)^{11}C$ reaction (Fig. 7), which has also a threshold below 1 MeV. To determine the proton energy one has to make additional exposures with absorbers in front of the boron target.

B. MONITOR REACTIONS FOR HEAVY IONS

At the 1969 Yerevan Conference the Russian team working on their electron-ring accelerator reported that they had accelerated nitrogen and produced ^{149}Tb in a cerium target. We have studied this and some other reactions for the purpose of monitoring heavy ions. Table II gives some of the selected reactions. We assumed that the ions listed are easy to inject or to produce in the electron ring.

1. Calculation of heavy-ion reaction cross sections

A program (CSPLOT) developed by Sikkeland was used for calculating heavy-ion reaction cross sections.[11] This program has been used successfully to calculate the production cross sections of nuclei formed by evaporation of three to eight neutrons from a compound nucleus. The program simply calculated the cross section $\sigma_x = \sigma_{cn} \cdot P_x$, where σ_{cn} is the cross section for the formation of the compound nucleus, and P_x is the probability of emission of x number of neutrons. Sikkeland's program uses for P_x an expression based on "Jackson's formula".[12]

For heavy elements, such as uranium, the competing fission reactions are also taken into account when calculating cross sections. We have chosen the program option to omit fission reactions on account of the medium-weight target elements we studied.

The parameters used in our calculations are those recommended by Sikkeland:

radius parameter	1.25×10^{-13} cm
nuclear potential	-70 MeV
diffusion parameter	0.46
I ratio	1.0
nuclear temperature	1.2 MeV.

Reaction Q values and binding energies for the first nine neutrons in the compound nucleus are taken from Myers and Swiatecki.[13]

The program CSPLOT calculates cross sections in mb and plots them on semilog paper. Figure 8 shows the results of one of these calculations. Cross sections are not normalized to the measured values. The comparison between measured and calculated cross-section values for the reaction $^{140}Ce(^{14}N, 5n)^{149}Tb$ is shown in Fig. 9. At the rising edge of the excitation curve there is agreement within the error limits between calculated and measured cross sections. Above threshold, the calculated curve rises faster than the experimental values, indicating that for the compound nuclei with high angular momentum, production of 4.1-h ^{149}Tb is lower than expected from the simple model. Four-min ^{149m}Tb is a strongly competing reaction channel for production of ^{149}Tb from heavy-ion interactions with cerium. Alexander and Simonoff[14] conclude that this isomer production is a very effective shield for inhibiting production of 4.1-h ^{149}Tb from the compound nuclei of high spin. Comparison of the calculations with experiments for the $^{140}Ce(^{14}N, 5n)^{149}Tb$ reaction should be possible for the low-energy portion of the excitation function, where the production cross section of ^{149m}Tb is low. It increases when partial waves with high angular momentum become important.

Table II gives some of the results of the calculations. The energy threshold is given for a cross section of 10^{-29} cm^2 for a target element with a single isotope. For other target elements the energy is given for a cross section of $10^{-29}/f$ cm^2, where f is the isotopic fraction of the target isotope considered.

From this energy threshold we obtain the approximate energy at which a measurable amount of radioactivity produced at saturation can be found. We have assumed a counting efficiency of 45%, a penetration length of about 10 mg/cm^2, and a decay rate of 5 dps, at which a measurement could be made with reasonable accuracy. For some reactions, however, we calculated the expected decay rate more precisely by taking into account both the penetration length of the heavy ion and the shape of the rising edge of the excitation curve.

We made the following calculations:

$$\text{production rate (dps)} = \frac{\phi f N}{A}\int_0^{E_{eff}} \sigma(E)\, SP(E,I)^{-1}\, dE$$

where

ϕ = ions/sec into target, assumed to be 10^{10} ions/sec,

f = fraction of isotope in target element,

N = Avogadro's number, 6.02×10^{23},

E_{eff} = minimum energy required to produce the necessary target activity,

A = atomic weight of target,

σ (E) = cross section in cm^2 from CSPLOT,

SP (E ,I) = stopping power as a function of ion energy and ion type.

From the above equation we get

$$8\times10^{-4}\,\frac{A}{I} = \int_0^{E_{eff}} \sigma_{mb}(E)\ (\text{mg/cm}^2)/\text{MeV}\ dE.$$

The values for E_{eff} which satisfy this equation are listed in Table II. Calculations were made for only a few reactions, and in these cases both the effective and threshold values agree closely. A comparison is made in the last columns between measured and calculated threshold energies for two reactions of given experimental cross sections. In these two cases, for which experimental cross-section values were available, the agreement between calculated and measured excitation energies on the rising part of the excitation curve is satisfactory.

Most of our effort has been directed towards the interaction of nitrogen ions with cerium targets. We were particularly interested in E_{eff} at which a measurable amount of 4.1-h ^{149}Tb could be produced. Before attempting to measure the cerium target exposed at the ERA, we ran a pilot exposure at the LRL 88-inch cyclotron at a known nitrogen ion energy.

2. 88-inch cyclotron pilot exposure

A thick cerium target, mounted as a charge integrator, was exposed to a beam of N^{+++} in the high-level cave of the LRL 88-inch cyclotron. The ion energy of 55.48 ± 0.5 MeV was determined precisely in a proton resonance spectrometer. During the 150 min of irradiation a charge of 2.41×10^{-3} coulomb (corresponding to 4.95×10^{15} ions) was collected on the Ce target. Following irradiation the activity of the Ce target was counted in a Frisch grid ion chamber α-particle spectrometer, and on a Ge(Li) γ-ray spectrometer.

a. Experimental results

Figure 10 gives the α-particle spectra obtained at different time intervals after irradiation; the background has been subtracted. It can be seen that a peak near channel 96 decays within a few hours whereas a smaller peak near channel 75 survives for a somewhat longer period. The total counts plotted against decay time are shown in Fig. 11. The counting rates are in good agreement with the assumption that two α-particle-emitting isotopes are present in the Ce target. The half-life of the first isotope lies between 4.1 and 4.2 h, and that of the longer-lived isotope between 17 and 18 h. The analysis of the data gives

(i) 8.3 cpm for the 18-h alpha activity, and

(ii) 42 cpm for the 4.2-h alpha activity.

With an α-particle counting efficiency of 45% we compute

(i) 3.4 dps for the 18-h activity, and

(ii) 4.6 dps for the 4.2-h activity.

The half-lives and channel locations of these activities suggest that they are due to ^{151}Tb and ^{149}Tb, respectively.

b. Estimation of the ^{149}Tb and ^{151}Tb production rates

Cerium has the following isotopes:

^{136}Ce	isotopic abundance	0.193%
^{138}Ce	isotopic abundance	0.25%
^{140}Ce	isotopic abundance	88.84%
^{142}Ce	isotopic abundance	11.07%.

From the calculations of the cross sections of reactions with various numbers of neutrons evaporated we can see that for the formation of ^{149}Tb with nitrogen bombardment, the compound nucleus ^{150}Tb would be too close to the desired end product (only one neutron evaporated) and the compound nucleus ^{156}Tb too far from it (seven neutrons evaporated). We have then only to consider production from ^{138}Ce and ^{140}Ce through the compound nuclei ^{152}Tb (three neutrons evaporated), and ^{154}Tb, respectively (five neutrons evaporated). The values for the integral

$$\text{dps} = \frac{\phi f N}{A} \int_0^E \sigma(E) \cdot SP(E,I)^{-1}\, dE$$

are given in Table III. It can be seen that the only appreciable amount of ^{149}Tb is produced from isotope ^{138}Ce, and of ^{151}Tb from isotope ^{140}Ce, for an energy limit of 55.48 MeV.

For an irradiation of 150 min and a constant flux of 5.5×10^{11} N^{+++}/sec we calculate the following production rates at saturation:

1. 12.4 α particles per sec for ^{149}Tb when an α-branching ratio of 0.226 is used,[15]

2. 1.86 α particles per sec for ^{151}Tb when an α-branching ratio of 8.3×10^{-5} is used.

The integrals were graphically evaluated and were found to be 9.15 mb(mg/cm^2) and 10.6 mb (mg/cm^2) for ^{149}Tb and ^{151}Tb, respectively.

The alpha-branching ratio for ^{151}Tb given in the compilation by Lederer, Hollander, and Perlman[10] and based on measurements made by McFarlane and Seegmiller[16] and Rasmussen, Thompson, and Ghiorso,[17] is 4.8×10^{-6}. It seems, however, from more recent evidence that this ratio might be too small. Recent measurements by Toth[18] give a branching ratio of $8.3\pm2.5\times10^{-5}$. We have adopted this latter value because our measurements of ^{151}Tb decay made with the Ge(Li) spectrometer tend to confirm it.

The ^{151}Tb production rate, also determined by the Ge(Li) measurements, is 2.85×10^4/sec. This compares well with the calculated value of 2.24×10^4. We compare in Table IV the calculated and measured values of ^{149}Tb and ^{151}Tb production and disintegration rates. We feel that the agreement is satisfactory. We are confident that we have found in this pilot experiment at least the two α-particle activities of ^{149}Tb and ^{151}Tb. We further see that the predictions made on the basis of calculated cross sections are reasonably accurate. Production of ^{149}Tb by nitrogen in cerium below 56 MeV (4 MeV/amu) is possible only through ^{138}Ce, which is 0.25% abundant in natural cerium.

At 55.48 MeV we have about 5 dps at saturation with a flux of 5×10^{11} ions/sec. This is about 50 times the minimum required to measure the alpha decay of ^{149}Tb. We estimate that at 56 MeV, at least 10^{14} nitrogen ions are needed to produce a significant amount of ^{149}Tb from ^{138}Ce.

Production of ^{149}Tb from ^{140}Ce isotope is about 10^3 times as great at 70 MeV as that from the same isotope at 56 MeV; it follows that at least 10^{11} nitrogen ions would be

required to produce a measurable amount of ^{149}Tb.

C. CERIUM TARGET EXPOSED IN THE ERA TEST RUN

During a 3-day test run at Livermore in December 1969, a 30-mm-thick elemental cerium target was exposed in the ERA acceleration tube. During this exposure it could not be established with certainty whether nitrogen ions were accelerated to 4 MeV/amu, nor could an estimation of beam intensity be made. The cerium target was counted at Berkeley 3 hours after irradiation. Our results were negative, thus indicating that less than 10^{14} nitrogen ions of 4 MeV/amu impinged on the target during the last 10 hours of exposure.

It was noted that our unirradiated foils exhibited unusually high alpha background on one side only. This activity may be due to thorium contamination of the foils, because cerium is found in minerals containing thorium.

D. CONCLUSIONS

It is possible to monitor heavy ions accelerated in the ERA by using suitable reactions leading to easily distinguishable α-particle emitters. Even at energies of about 5 MeV/amu a total of about 10^{11} ions would be needed to produce a measurable amount of α-particle activity. Short-lived isotopes can be used in arrangements allowing remote removal of the irradiated target to a shielded counting facility, preferably inside the ERA vacuum.

Monitor reactions of the type described can also be used to measure the composition of the residual gas in ERA. With different ions, different alpha emitters can be produced simultaneously.

Preliminary experiments at the ERA (December 1969) have shown that less than 10^{14} nitrogen ion were accelerated to $\geq$4 MeV/amu.

REFERENCES

1. D. Keefe, Research on the Electron Ring Accelerator, Particle Accelerators, Vol. 1, 1-13 (1970).
2. G. R. Choppin, J. R. Meriwether, and J. D. Fox, Phys. Rev. 131, 2149 (1963).
3. G. A. Tewes and R. A. James, Phys. Rev. 88, 860 (1952).
4. J. P. Butler, B. J. Bowles, and F. Brown, in Proceedings of the Second United Nations International Conference on Peaceful Uses of Atomic Energy, Geneva, Switzerland, 1958, Vol. 15, p. 156.
5. W. R. Jones, A. Timmick, J. H. Paehler, and T. H. Handley, Phys. Rev. 99, 184 (1955).
6. E. K. Hyde, The Nuclear Properties of Heavy Elements, Vol. III (Prentice-Hall, 1964), pp. 72, 493.
7. F. Ajzenberg and T. Lauritsen, Rev. Mod. Phys. 27, 77 (1955).
8. G. A. Sawyer and J. A. Phillips, Survey of Several of the Reactions Occurring When Lithium and Beryllium are Bombarded by Protons and Deuterons of 30-250 keV, Los Alamos Report 1578, 1953.
9. R. J. Howerton, D. Braff, W. J. Cahill, and N. Chazan, Thresholds of Nuclear Reactions, UCRL-14000, 1964.
10. C. M. Lederer, J. M. Hollander, and I. Perlman, Table of Isotopes, Sixth Edition (John Wiley and Sons Inc., New York, 1967).
11. T. Sikkeland, J. Maly, and D. H. Lebeck, Phys. Rev. 169, 1000 (1968).
12. J. D. Jackson, Can. J. Phys. 34, 767 (1956).
13. W. D. Myers and W. J. Swiatecki, Tables of Nuclear Masses and Deformations, UCRL-11980, 1965.
14. J. M. Alexander and G. N. Simonoff, Phys. Rev. 130, 2383 (1963).

15. Y. Y. Chu, E. M. Franz, and G. Friedlander, Phys. Rev. 175, 4 (1968).
16. R. D. Macfarlane and D. W. Seegmiller, Nucl. Phys. 53, 449 (1964).
17. J. O. Rasmussen, Jr., S. G. Thompson, and A. Ghiorso, Phys. Rev. 89, 33 (1953).
18. K. S. Toth, Nucl. Phys. 133A, 222 (1969).

Table I. Reactions used for proton monitoring.

Reaction	Threshold[a] (MeV)	Branching[b] ratio	Half-life[b]	Target
$^{11}B(p,n)^{11}C$	3.02	1.0	20.34 min	Boron
$^{14}N(p,n)^{14}O$	3.78	1.0	70.91 sec	NH_4F
$^{18}O(p,n)^{18}F$	2.59	1.0	109.7 min	BeO
$^{43}Ca(p,n)^{43}Sc$	3.07	0.88	3.92 h	CaO
$^{45}Sc(p,n)^{45}Ti$	2.90	0.84	3.09 h	Sc
$^{47}Ti(p,n)^{47}V$	3.77	1.0	33 min	Ti
$^{19}F(p,n)^{19}Ne$	4.24	1.0	17.4 sec	LiF

[a]From Ref. 8.
[b]From Ref. 9.

Table II. E_{th} from program CSPLOT, E_{eff} calculated for 5 dps at saturation with 10^{10} ions/sec.

Ion			Target			f	Number neutrons out	Produced			Half-life	σ (mb)	E_{th} (MeV)	E_{eff} (MeV)	MeV/amu	σ (mb)	Energy Measured (MeV)	Energy Calculated (MeV)
	Z	A		Z	A				Z	A								
Li	3	7	Sm	62	144	0.031	2	Tb	65	149	4.1 h	0.32	19	19.6	2.80			
C	6	12	Sm	62	144	0.031	2	Er	68	154	5 min	0.32	46	46.5	3.88			
C	6	12	Nd	60	142	0.27	3	Dy	66	151	18 min	0.04	47		3.92	56	54	52
N	7	14	Nd	60	142	0.27	4	Ho	67	152	2.4 min	0.04	56		4.00			
N	7	14	Ce	58	138	0.0025	3	Tb	65	149	4.1 h	4.0	54	56.5	4.04			
N	7	14	Ce	58	140	0.89	5	Tb	65	149	4.1 h	0.011	62		4.4	11	67	68
O	8	16	Pr	59	141	1.0	5	Ho	67	152	2.4 min	0.01	76		4.75			
O	8	16	Nd	60	142	0.27	4	Er	68	154	5 min	0.04	68		4.25			
							5	Er	68	153	36 sec	0.04	82		5.12			
Ne	10	20	Cs	55	133	1.0	4	Tb	65	149	4.1 h	0.01	71	72.3	3.62			
Ne	10	20	La	57	139	1.0	7	Ho	67	152	2.4 min	0.01	110		5.50			
Ne	10	20	Mo	52	92	0.16	4	Te	52	108	5.3 sec	0.063	80		4.00			
							5	Te	52	107	2.2 sec	0.063	96		4.80			
A	18	40	Cd	48	112	0.24	3	Dy	66	149[a]	10-20 min	0.04	137	141	3.52			
A	18	40	Sm	50	116	0.14	3	Er	68	153	36 sec	0.072	142		3.55			
							4	Er	68	152	10.7 sec	0.072	139		3.48			

[a]^{149}Dy then decays into 4.1-hr ^{149}Tb.

Table III. Ce(N, spall) Tb, Cross section and stopping power.

$E(N^{+++})$ (MeV)	Stopping power $\left(\frac{MeV}{mg/cm^2}\right)$	$^{138}Ce \rightarrow {}^{149}Tb$ σ (mb)	σ/SP	$^{140}Ce \rightarrow {}^{151}Tb$ σ (mb)	σ/SP	$^{140}Ce \rightarrow {}^{149}Tb$ σ (mb)	σ/SP	$^{138}Ce \rightarrow {}^{151}Tb$ σ (mb)	σ/SP
45	2.115	7.84×10^{-5}	3.71×10^{-5}	8.69×10^{-5}	4.11×10^{-5}	$<10^{-12}$		3.69×10^{-6}	1.74×10^{-6}
46	2.095	5.27×10^{-4}	2.52×10^{-4}	6.076×10^{-4}	2.90×10^{-4}	$<10^{-12}$		4.86×10^{-6}	2.32×10^{-6}
47	2.075	2.42×10^{-3}	1.16×10^{-3}	2.85×10^{-3}	1.37×10^{-3}	$<10^{-12}$		6.36×10^{-6}	3.06×10^{-6}
48	2.055	8.96×10^{-3}	4.36×10^{-3}	1.07×10^{-2}	0.52×10^{-2}	$<10^{-12}$		8.27×10^{-6}	4.02×10^{-6}
49	2.035	2.71×10^{-2}	1.33×10^{-2}	3.27×10^{-2}	1.61×10^{-2}	$<10^{-12}$		9.26×10^{-6}	4.55×10^{-6}
50	2.020	8.09×10^{-2}	4.00×10^{-2}	9.85×10^{-2}	4.87×10^{-2}	$<10^{-12}$		1.20×10^{-5}	5.93×10^{-6}
51	1.995	2.3×10^{-1}	1.15×10^{-1}	2.81×10^{-1}	1.40×10^{-1}	$<10^{-12}$		1.54×10^{-5}	7.72×10^{-6}
52	1.980	6.29×10^{-1}	3.17×10^{-1}	7.75×10^{-1}	3.91×10^{-1}	$<10^{-12}$		1.97×10^{-5}	0.99×10^{-5}
53	1.960	1.67	0.852	2.07	1.06	$<10^{-12}$		2.51×10^{-5}	1.28×10^{-5}
54	1.940	4.31	2.22	5.31	2.74	$<10^{-12}$		3.11×10^{-5}	1.60×10^{-5}
55	1.920	10.48	5.46	12.8	6.66	$<10^{-12}$		3.71×10^{-5}	1.93×10^{-5}
56	1.900	22.55	11.87	29.5	15.5	$<10^{-12}$		4.03×10^{-5}	2.12×10^{-5}
57	1.880	44.32	23.57	50.7	26.9	$<10^{-12}$		4.44×10^{-5}	2.36×10^{-5}
58	1.865	69.63	37.04	76.8	40.85	$<10^{-12}$		4.16×10^{-5}	2.21×10^{-5}
59	1.845	90.15	48.86	108	58	$<10^{-12}$		2.07×10^{-5}	1.12×10^{-5}
60	1.825	101.3	55.50	120	65.8	$<10^{-12}$		5.12×10^{-6}	2.81×10^{-6}
61	1.805					7.86×10^{-13}	4.4×10^{-13}		
62	1.785					3.95×10^{-5}	2.18×10^{-5}		
63	1.765					6.55×10^{-3}	3.71×10^{-3}		
64	1.745					1.13×10^{-1}	0.643×10^{-1}		
65	1.730					7.53×10^{-1}	4.35×10^{-1}		
66	1.710					2.96	1.73		
67	1.690					8.34	4.93		
68	1.670					18.7	11.19		
69	1.650					35.5	21.5		
70	1.630					59.6	36.6		

Table IV. Production and disintegration rates.

Isotope	Calculated production rate[a] (dps)	Ge(Li) measured production rate (dps)	Alpha branching ratio taken from the literature	Calculated alpha disintegration rate (dps)	Measured alpha disintegration (dps)
^{149}Tb	55		0.226(15)	12.4	4.6
^{151}Tb	22 400	28 500[b]	8.3×10^{-5}(18)	1.86	3.4

[a]Based on saturated activity and a flux of 5.5×10^{11} N^{+++}/sec.

[b]Based on gamma transition intensities taken from Toth, Ref. 18.

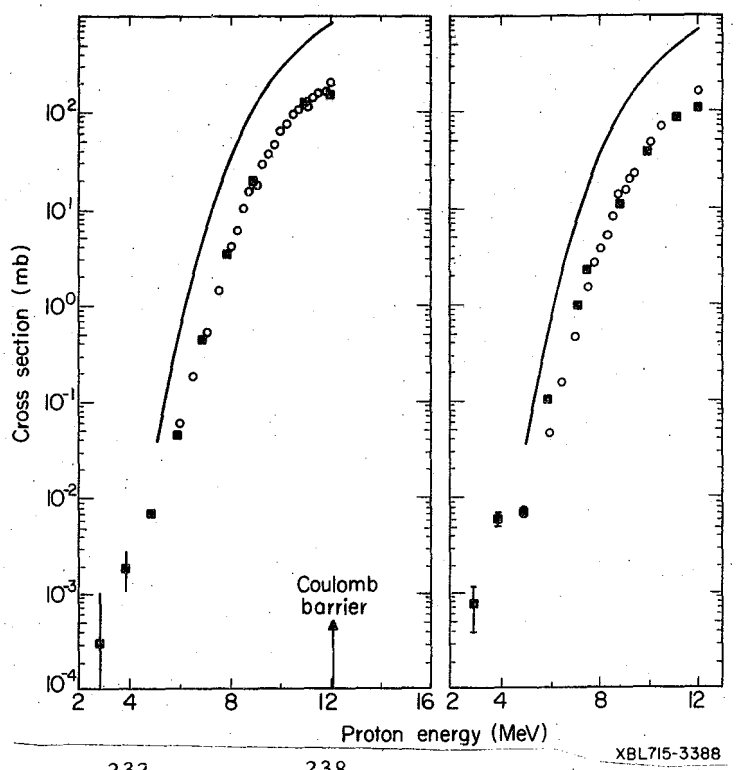

Fig. 1. ^{232}Th(p, f) and ^{238}U(p, f) excitation functions (from Choppin et al., Ref. 2.
O Junction counter data.
■ recoil catcher data,
— total reaction cross section (optical model).

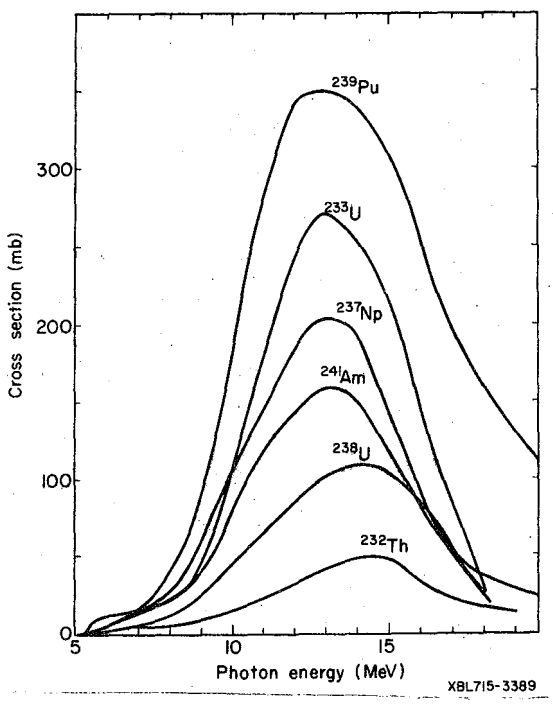

Fig. 2. Photofission cross sections versus photon energy (after Hyde, Ref. 6).

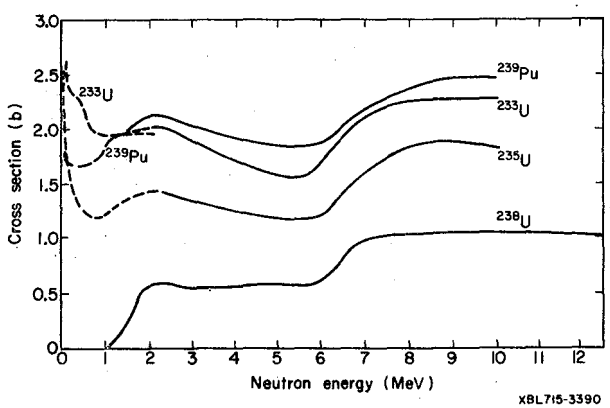

Fig. 3. Variation of fission cross section with fast neutron energy (after Hyde, Ref. 6).

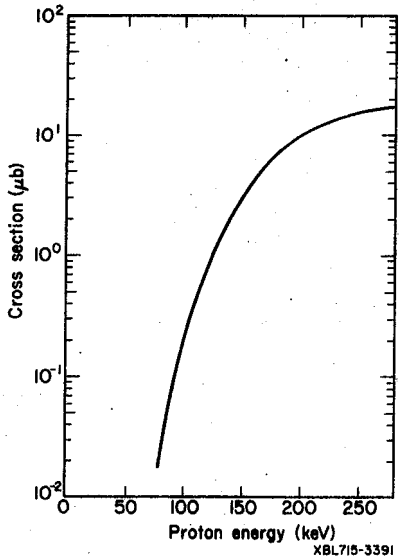

Fig. 4. $^{7}Li(p,\gamma)^{8}Be$ excitation function at low proton energies (Q = 17.242 MeV) (see Refs. 7 and 8).

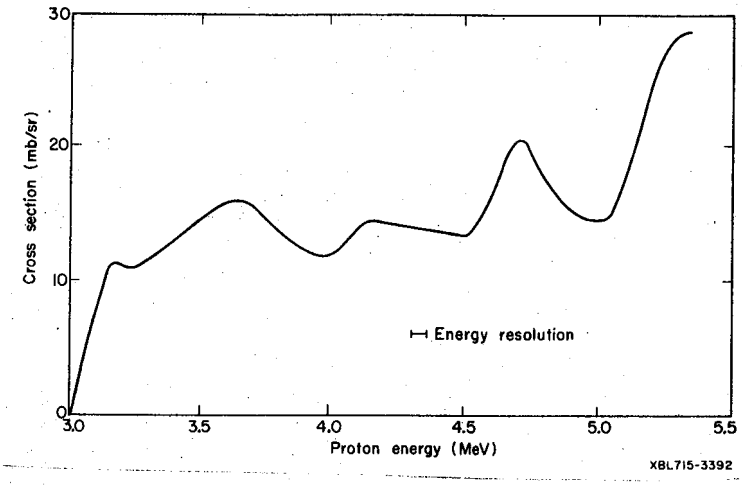

Fig. 5. $^{11}B(p,n)^{11}C$ excitation function. Lab angle 0 to 10 deg. (Taken from Los Alamos Report LA-2014.)

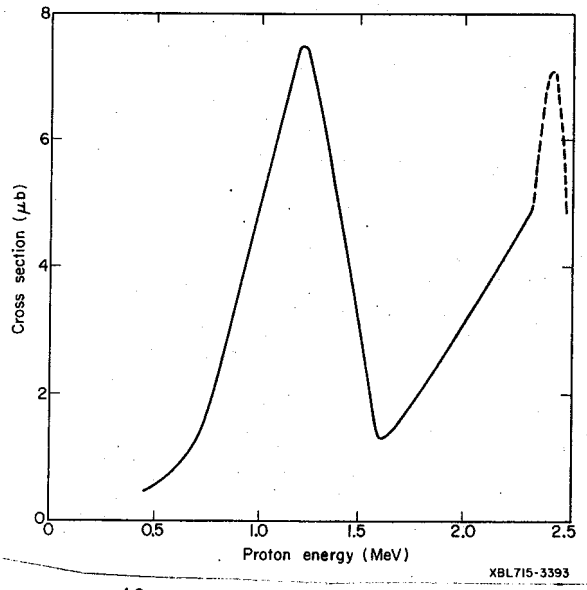

Fig. 6. $^{10}B(p,\gamma)^{11}C$ excitation function. (From Los Alamos Report LA-2014.)

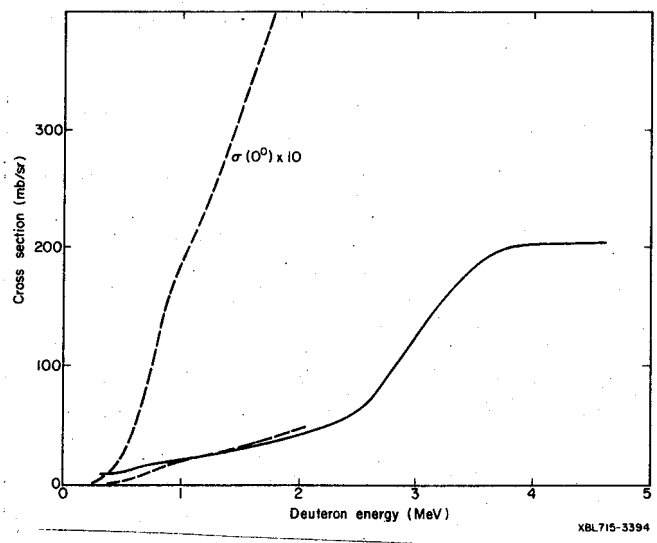

Fig. 7. $^{10}B(d,n)^{11}C$ excitation function. Lab angle 0 deg. (Taken from Los Alamos Report LA-2014.)

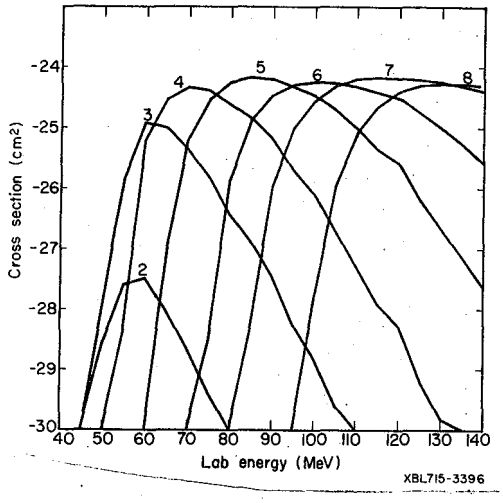

Fig. 8. Drawing derived from typical CSPLOT output, showing the production of ^{154}Tb from ^{14}N on ^{140}Ce. Numbers above each curve indicate number of evaporated neutrons; curve labeled 5 indicates the cross section for production of ^{154}Tb with subsequent evaporation of five neutrons, leading to ^{149}Tb.

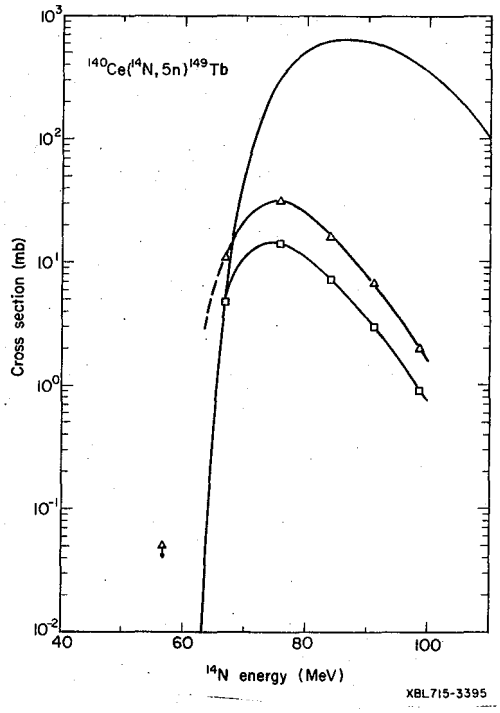

Fig. 9. Comparison between calculated (CSPLOT) cross-section values (which include ^{149m}Tb production) for the reaction ^{140}Ce(^{14}N, 5n)^{149}Tb and measured values adjusted for two different values of the α-branching ratio.

— CSPLOT calculation; includes ^{149m}Tb production.

△ Measured, ^{149}Tb only (Ref. 14). Data multiplied by 1/a; a = branching ratio = 0.1.

□ Data of △ adjusted to an α-branching ratio of 0.226 (Ref. 15).

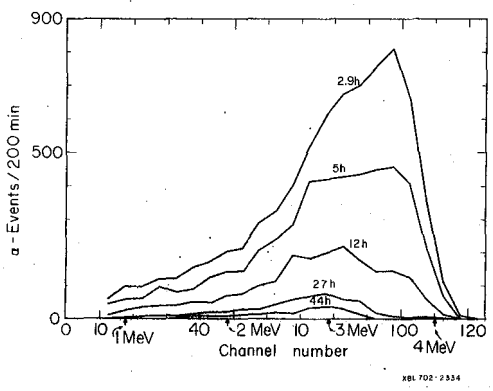

Fig. 10. Alpha spectra at decay times from 2.9 to 44 hr from cerium bombardment with $^{14}N^{+++}$ at 55.48 MeV at the LRL 88-inch cyclotron.

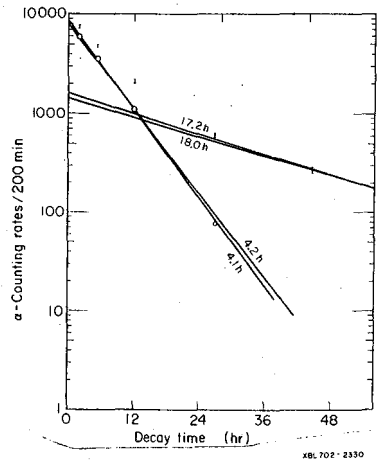

Fig. 11. Alpha-particle counting rates from cerium irradiation, indicating presence of two α-emitting isotopes.